HOXA5 inhibits the proliferation and metastasis of cervical squamous cell carcinoma by suppressing the β-catenin/Snail signaling

Wan-Yu JIN[1,2,#], Yan ZHANG[1,#], Jia TIAN[1], Long-Kuan XU[1], Heng-Jie LIN[2], Yu-Zhong YANG[1], Xue-Mei ZHANG[1], Mei-Hua JIN[1], Wen-Fa MO[1], Guang-Ying QI[3], Ying-Qiong ZHOU[1,*]

[1]Department of Pathology, Affiliated Hospital of Guilin Medical University, Guilin, Guangxi, China; [2]Faculty of Basic Medical Sciences, Guilin Medical University, Guilin, Guangxi, China; [3]Key Laboratory of Tumor Immunity and Microenvironment Regulation, Guilin Medical University, Guilin, Guangxi, China

*Correspondence: 15977321166@163.com; 631375867@qq.com
#Contributed equally to this work.

HOXA5, as a transcription factor, plays an important role in a variety of malignant tumors. Nevertheless, its biological role in cervical squamous cell carcinoma (CSCC) is largely unknown. In our study, we aimed to explore the function of HOXA5 in CSCC and its molecular mechanism. Immunohistochemistry showed that HOXA5 expression was downregulated in human CSCC tissues and HOXA5 staining was negatively correlated with tumor size and histological grade of CSCC. Ectopic expression of HOXA5 inhibited proliferative and metastatic abilities of CSCC cells in vitro and in vivo. Furthermore, overexpression of HOXA5 inhibited the cell cycle by arresting the S/G2 phase by flow cytometry and that was related to the downregulation of Cyclin A. Further study showed that HOXA5 suppressed EMT by inhibiting the β-catenin/Snail signaling resulting in reduced metastasis of CSCC cells. Altogether, our results suggested that HOXA5 inhibited the proliferation and metastasis via repression of the β-catenin/Snail pathway, proposing the potential role of HOXA5 in the prevention and treatment of CSCC.

Key words: HOXA5; cervical squamous cell carcinoma (CSCC); EMT; β-catenin; Snail

Cervical carcinoma is a common malignancy, which ranks fourth in both morbidity and mortality in all cancer types in females all over the world [1]. Although with the development of early screening, HPV vaccination, surgery, radiotherapy, and chemotherapy, morbidity and mortality have reduced in developed countries, there is a lack of early screening in developing countries [2]. Cervical carcinoma has a poor prognosis due to local invasion and lymphatic metastasis, threatening women's health and lives seriously [3]. There are multiple factors that contribute to the development of cervical carcinoma, including HPV infection, genetic changes, environmental factors, etc. Cervical squamous cell carcinoma (CSCC) is the main pathological type of cervical carcinoma, accounting for about 85% of the total number of cases [4]. Hence, there is a compelling need to explore the underlying mechanism during the progression and metastasis of CSCC.

Homeobox (HOX) genes are a highly conserved family of transcription factors that regulate embryonic development and cell differentiation [5, 6]. Their expression is strictly temporal and spatial specificity, and aberrant expression is associated with the occurrence and development of malignant tumors [7]. HOX genes have been reported to play an important role in the progress of various cancers, such as breast cancer, lung cancer, colon cancer, thyroid cancer, and leukemia [8, 9]. HOXA5 is a member of HOX gene family and is a transcriptional factor that participates in regulating organ development [8]. Aberrant expression of HOXA5 is reported to correlate with many cancers, such as breast carcinomas [10], gastric cancer [11], renal cancer [12], melanoma [13], and colorectal cancer [14]. In our previous study, HOXA5 is downregulated in CSCC compared to chronic cervicitis and low expression of HOXA5 correlates with a worse prognosis [15]. However, the molecular mechanisms of HOXA5 in the development of CSCC are mostly unclear.

In this study, we demonstrate that HOXA5 is downregulated in CSCC lesions and ectopic expression of HOXA5 inhibits the proliferation, invasion, and metastasis of CSCC cells by suppressing the β-catenin/snail signaling pathway.

Patients and methods

Clinical samples. A total of 315 CSCC tissues and adjacent tissues from the year 2013 to 2020 were collected from the Department of Obstetrics and Gynecology, the First Affiliated Hospital and the Second Affiliated Hospital of Guilin Medical University. All these patients did not receive radiotherapy, chemotherapy, or immunotherapy prior to the operation. Written informed consent was obtained from each patient. The study was approved by the Ethics Committee of the Affiliated Hospital of Guilin Medical University (the approval Ethics ID 2017KJT-15). The patients' ages range from 24 to 78. The tissues were collected during the operation and stored at –80 °C for western blotting assay. The paraffin-embedded tissues were collected to make tissue chips and immunohistochemistry.

Cell lines and cell culture. The human cervical cancer cell lines SiHa and CaSki were obtained from the Cell Resource Center, Shanghai Institutes of Biological Sciences, Chinese Academy of Sciences. SiHa cells were grown in high glucose Dulbecco Modified Eagle Medium (DMEM, Gibco, C11995500BT) and CaSki cells were cultured with RPMI-1640 Medium (Gibco, C11875500BT) supplemented with 10% FBS (Cyagen, FBSST-01033) and 1% penicillin-streptomycin (Solarbio, P1400) at 37 °C with 5% CO_2.

Transient transfection and lentivirus infection. The plasmid pcDNA3.1-HOXA5 was obtained from Addgene. Transient transfection of plasmids was operated according to the manufacturer's manual by using Lipofectamine 3000 reagent (Thermo Fisher, L3000015). In brief, 3 μg plasmid or 4.5 μl Lipofectamine 3000 were blended with Opti-MEM (Gibco, 31985070), respectively. Then, these two regents were mixed slowly, incubated for 20 min, and added to cells. The HOXA5 expression was verified by western blotting. The lentivirus system was kindly presented from Wu's lab, which contained four plasmids: pLVX-mCherry-N1, pLP1, pLP2, and pLP/VSVG [16]. HOXA5 was inserted into pLVX-mCherry-N1. For packaging lentivirus, 8 μg recombinant plasmid pLVX-mCherry-N1-HOXA5, 5.8 μg pLP1, 2.4 μg pLP2, and 5.8 μg pLP/VSVG were transfected into 100 mm plate of 293T cells. The cellular supernatants were collected after 48 h and 72 h and condensed with PEG-8000 overnight and centrifuged to collect the lentivirus. We infected SiHa and CaSki cells with lentivirus carrying HOXA5 coding sequence and added puromycin (Solarbio, P8230) to select infected cells. The living cells were cultured in DMEM with 10% FBS and the HOXA5 expression was detected by western blotting. The cells stably overexpressing HOXA5 were established.

Hematoxylin-Eosin staining and immunohistochemistry. The human tissues, mice xenograft tumors, and lung tissues were fixed by 10% formaldehyde, dehydrated, embedded in paraffin, and sectioned into 4 μm slices for H&E staining and immunohistochemistry. As to H&E staining, the paraffin sections were dewaxed, rehydrated, and stained with hematoxylin and eosin. For immunohistochemistry, the

paraffin sections were dewaxed, rehydrated, and antigens were retrieved, then blocked with 3% hydrogen peroxide for 10 min and normal goat serum for 1 hour at room temperature. The sections were incubated with anti-HOXA5 (Abcam, ab82645), anti-Ki-67 (Maxim Biotechnologies, MAB-0672), anti-E-cadherin (Abcam, ab40772), anti-N-cadherin (Abcam, ab76011), anti-β-catenin (Abcam, ab231305), anti-Snail (Affinity, AB-2834965), and anti-Vimentin (Affinity, AB-2847777) antibodies at 4 °C overnight and secondary antibody conjugated HRP-Polymer (Maxim Biotechnologies, KIT-5230) for 20 min. The staining was visualized 3,3-diaminobenzidine (DAB, Maxim Biotechnologies, DAB-1031) and counterstained with hematoxylin. Five random photos were captured from each section. According to the staining intensity, negative staining scored 0, light yellow staining scored 1, yellow staining scored 2, and brown staining scored 3. Based on the percentage of positive cells, no positive cell staining scored 0, <10% scored 1, 11–50% scored 2, 51–75% scored 3, and >75% scored 4. Then the evaluation was determined by multiplying scores of intensity and percentage. A score less than 3 was designated as negative and a score 3 as positive.

Western blotting. Tissues or cells were lysed by RIPA tissue/cell lysate (Solarbio, R0010) addition with PMSF (Solarbio, P0100) and protease inhibitor, and proteins were extracted after centrifugation. The protein was quantified with a BCA protein concentration determination kit (Beyotime Biotechnology, P0010S). After loading 40 micrograms of lysates into gels, sodium dodecyl sulfate-polyacrylamide gel electrophoresis (SDS-PAGE) was used to separate proteins, and then transferred onto the polyvinylidene difluoride (PVDF) membrane (Merck Millipore, IPVH00010). Nonspecific binding was blocked by 5% skim milk at room temperature for 1 h. The membranes were incubated with anti-HOXA5, anti-E-cadherin, anti-N-cadherin, anti-β-catenin, anti-Snail, anti-Vimentin, anti-Cyclin A (Cell Signaling Technology, 4656), anti-GAPDH (Affinity Biosciences, AB-2839421), and anti-Tubulin, (Affinity Biosciences, AB-2827688) at 4 °C overnight and incubated with HRP-labeled goat anti-rabbit IgG (Affinity Biosciences, S0002) or anti-mouse IgG (Affinity Biosciences, S0001) at room temperature for 1 h. The proteins were detected by using an ECL reagent (Affinity Biosciences, KF005). The proteins were quantitatively analyzed by ImageJ software. Each experiment was repeated three times independently.

Cell proliferation test. Cell counting kit-8 (CCK-8, Bimake, B34302) and colony formation assay was performed to test cell proliferation activity according to standard procedures. Briefly, as CCK-8 assay; 2,000 cells were seed in a 96-well plate and 10 μl CCK-8 were added in each hole and incubated for 3 h. The absorbance (OD) values were read using a microplate reader (Bio-Rad) at a wavelength of 450 nm. The CCK-8 assay was tested every 24 h for 5 days. As colony formation assay; 1,000 cells were seed in a 6-well plate and cultured for 10 days to form cell colonies. The cells were fixed with 4% paraformaldehyde and stained

with crystal violet. The numbers of colonies were counted by ImageJ software. Each experiment was repeated three times independently.

Cell migration and invasion test. A wound healing assay was used to test the migration ability. The cells were plated in 6-well plates to form a full layer and scratched by 10 μl tips. Migrated cells were observed under a microscope at 0 h, 24 h, and 48 h. Transwell assay without Matrigel (BD Biosciences, 356234) was also to detect cell migration ability, and Transwell assay with Matrigel was used to test the cell invasion ability. 1×10^4 cells were added to the upper Transwell chamber (Corning, 3422) and DMEM with 10% FBS was added to the lower chamber. The migrated or invaded cells in the lower chamber were fixed with 4% paraformaldehyde and stained with crystal violet. The cells were observed under a microscope (Olympus). Each experiment was repeated three times independently.

Flow cytometry analysis. The cell cycle was measured by using a cell cycle detection kit (Beyotime Biotechnology, C1052). Cells were harvested by centrifugation and fixed with pre-cooled 70% ethanol for 30 min at 4 °C and then incubated with 25 μl PI and 10 μl RNaseA for 30 min at 37 °C. Cell cycle distribution was quantified by BD FACS Canto™ (BD Biosciences, USA). Data were analyzed with the FlowJo software. Each experiment was repeated three times independently.

Xenograft tumor in nude mice. Four-week-old female nude mice (BALB/c) were purchased from Hunan SJA Laboratory Animal Co., Ltd. (Changsha, China). The mice were fed in a specific pathogen-free condition where the temperature is at 22–25 °C and the humidity is at 40–50%. The animal experiments were approved by the Animal Ethics Committee of Guilin Medical University (The approval Ethics ID GLMC-IACUC-2021014). The mouse protocols were performed in accordance with the guidelines for the care of laboratory animals and the Animal Care and Use Committee of Guilin Medical University. To test the SiHa-mCherry and SiHa-mCherry-HOXA5 cells' ability to grow in nude mice, 16 mice were divided randomly into two groups. 1×10^6 cells in 100 μl PBS were injected into subcutaneous on the back of nude mice and the tumor volume was measured every 4 days. After 33 days, the nude mice were sacrificed and the tumor tissues were separated to measure the size and weight. To test the two cell types' migration ability in nude mice, 16 mice were divided randomly into two groups. 2×10^5 cells in 200 μl PBS were injected into the tail intravenous and the lung tissues were separated to measure the number of metastases after 40 days.

Statistical analysis. Statistical analysis was conducted by using GraphPad Prism version 8.0 software and SPSS version 17.0 software. Quantitative data were presented as the mean ± standard deviation (SD). Comparisons between two groups were determined by the unpaired t-test, and comparisons among multiple groups were performed using ANOVA. The relationship between HOXA5 expression and clinic patho-logical factors were analyzed using Spearman correlation analysis. A p-value of <0.05 was considered to indicate a statistically significant. Each experiment was repeated three times independently.

Results

HOXA5 is significantly downregulated in CSCC tissues. To explore the expression of HOXA5 in CSCC, we used western blotting to detect HOXA5 expression in CSCC and relevant adjacent cervical tissues and the results showed that the HOXA5 protein was significantly less in CSCC tissues than relevant adjacent cervical tissues (Figures 1A, 1B). Tissue microarrays including human CSCC tissues (n=212) and non-cancerous control tissues (para-carcinoma and normal tissues, n=103) were utilized to detect the expression of HOXA5. Immunohistochemistry results showed that HOXA5 mainly localized in the cytoplasm and the expression of HOXA5 was significantly downregulated in CSCC tissues compared to non-cancerous control tissues (p<0.05, Figure 1C). The proportion of tissues, which were positive staining of HOXA5 was 73.8% in non-cancerous control tissues but 60.0% in CSCC tissues (Figure 1D). Then we analyzed the relationship between the expression of HOXA5 and the clinicopathology of CSCC patients. As shown in Table 1, the expression of HOXA5 was negatively correlated

Table 1. The relationship between HOXA5 and clinicopathological of CSCC.

| Clinicopathologic parameters	Expression of HOXA5			
	Number of cases	Positive (+)	Negative (−)	p-value
CSCC	212	125 (60.0)	87 (40.0)	0.010
Non-cancerous control	103	76 (73.8)	27 (26.2)	
Age (years)				
<49	104	59 (56.7)	45 (43.3)	0.800
≥49	94	55 (58.5)	39 (41.5)	
Tumor size (cm)				
<3	75	51 (68)	24 (32)	0.004
≥3	62	27 (43.5)	35 (56.5)	
Histological grade				
Well differentiation	48	31 (64.6)	17 (35.4)	0.031
Moderate differentiation	74	46 (62.2)	28 (37.8)	
Poor differentiation	79	35 (44.3)	44 (55.7)	
Infiltrate the muscle layer				
Yes	110	68 (61.8)	42 (38.2)	0.003
No	38	13 (34.2)	25 (65.8)	
Lymph node metastases				
Yes	17	10 (58.8)	7 (41.2)	0.600
No	102	53 (52.0)	49 (48.0)	
Overall survival				
<5 years	6	4 (66.7)	2 (33.3)	0.434
≥5 years	68	34 (50.0)	34 (50.0)	
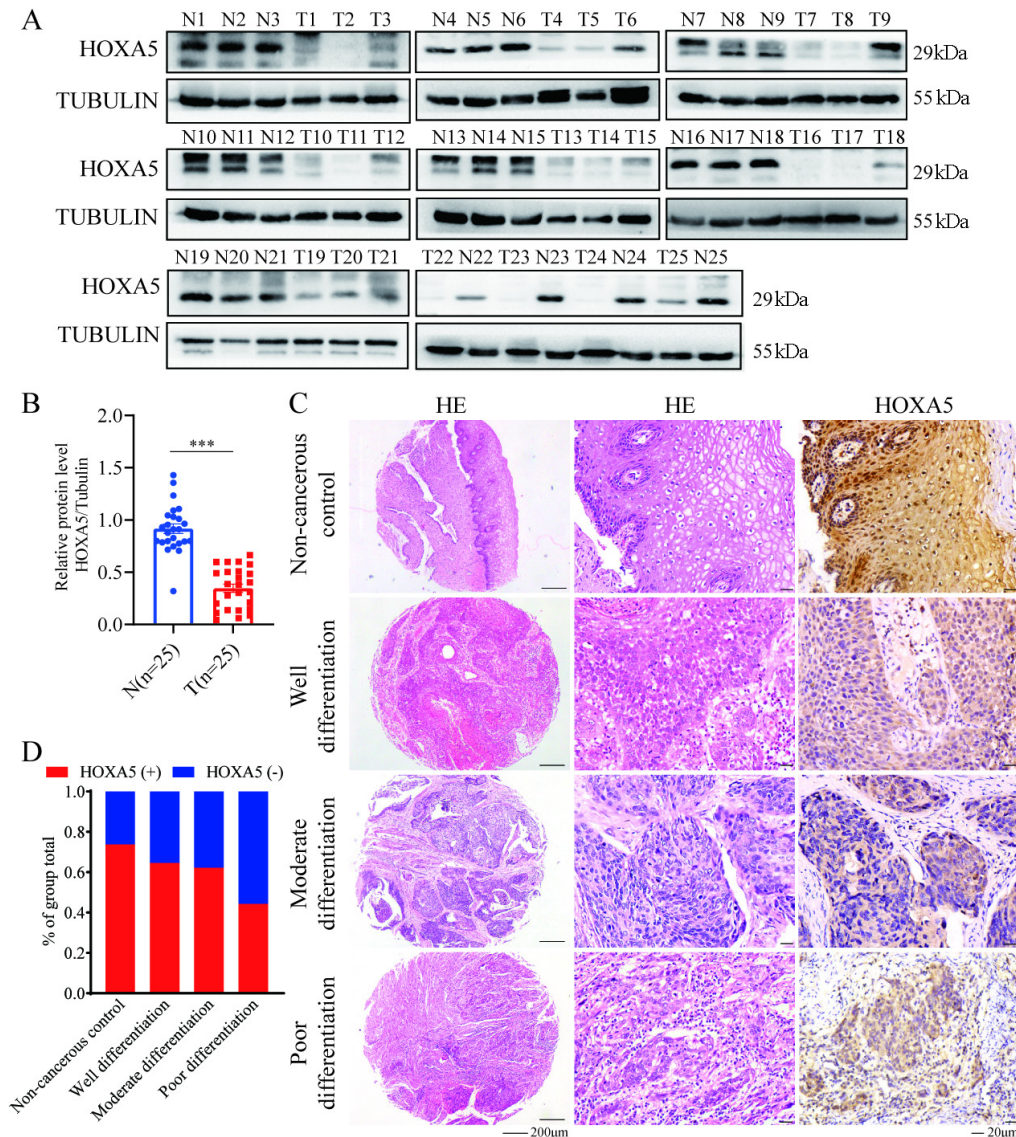
Figure 1. HOXA5 was significantly downregulated in CSCC tissues. A) HOXA5 levels were detected by western blotting in 25 cases of fresh CSCC and para-carcinoma tissues (N, para-carcinoma tissues; T, tumor tissues). **B)** Quantification of western blotting bands by ImageJ software, and the ratios of HOXA5 to tubulin were used to draw the figure. The expression of HOXA5 in CSCC and its corresponding para-carcinoma tissues were shown. (***p<0.001). **C, D)** The expression of HOXA5 was detected by immunohistochemical staining in CSCC tissues and non-cancerous control group tissues.

with tumor size and histological grade of CSCC. These results indicated that the expression of HOXA5 was downregulated in CSCC, which suggested that HOXA5 may play an important role in the progression of CSCC.

Ectopic expression of HOXA5 suppresses the proliferation, migration, and invasion of CSCC cells *in vitro*. The expression of HOXA5 in CSCC cell lines was evaluated by western blotting. As shown in Figure 2A, HOXA5 showed low or even no expression in SiHa and CaSki cells. To investigate the role of HOXA5 in CSCC cells, we overexpressed HOXA5 in SiHa and CaSki cells. The expression of HOXA5

was verified by western blotting (Figures 2B, 2C). CCK-8 and clone formation assays demonstrated that SiHa and CaSki cells overexpressing HOXA5 (CaSki-OE-HOXA5, SiHa-mCherry-HOXA5) exhibited markedly lower proliferation ability than their control cells (CaSki-pcDNA3.1, SiHa-mCherry) (Figures 2D–2F). Moreover, wound healing and Transwell assays indicated that overexpression of HOXA5 decreased the migration and invasion abilities in SiHa and CaSki cells (Figures 2G–2J). These results suggested that HOXA5 inhibited CSCC cell proliferation, migration, and invasion *in vitro*.
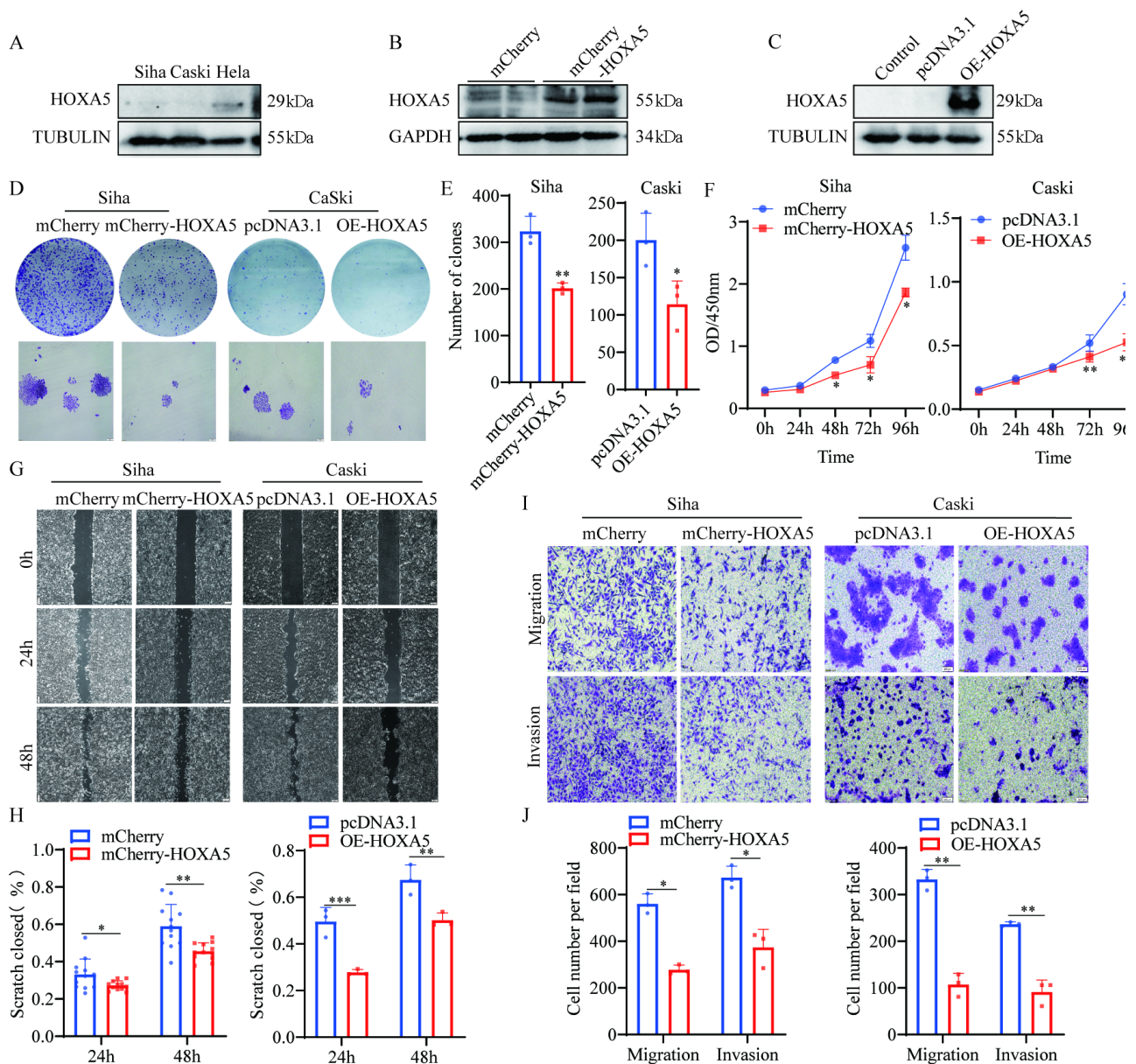
Figure 2. Ectopic expression of HOXA5 suppresses the proliferation, migration, and invasion of CSCC cells *in vitro*. A) The expression of HOXA5 in CSCC cell lines was detected by western blotting. **B, C)** The HOXA5 levels were detected by western blotting when ectopic expression of HOXA5 in SiHa cells (B) and CaSki cells (C). **D)** The cell proliferation capacity was measured by clone formation assay. **E)** The number of colonies was counted to make the chart. **F)** The cell proliferation abilities were conducted by CCK-8 assay in SiHa and CaSki cells. **G)** The migration abilities were measured by wound healing assay. **H)** The ratio of wound healing was calculated by the unclosed area minus the original area. **I)** The migration and invasion abilities were measured by Transwell assays with or without matrigel respectively. **J)** The number of cells that migrated to lower chambers was counted by ImageJ software. Each experiment was independently performed three times (*p<0.05, **p<0.01, ***p<0.001).

HOXA5 arrests the cell cycle from S to G2 phase. To investigate the mechanism of HOXA5 inhibited the proliferation of CSCC cells, flow cytometry was performed to analyze the cell cycles of HOXA5-OE cells and control cells. As shown in Figures 3A and 3B, overexpression of HOXA5 led to a decrease in the percentage of cells cycle in the G0/G1 phase (60.25±4.69% vs. 21.68±1.96%, p<0.001), but an increase in

the S phase (26.08±1.57% vs. 64.66±6.07%, p<0.001) in SiHa cells. Similar results were obtained from CaSki cells with the G0/G1 phase (45.77±0.55% vs. 31.52±0.23%, p<0.001) and the S phase (39.78±0.12% vs. 56.70±3.04%, p<0.001). These results suggested that HOXA5 inhibited the proliferation of CSCC cells by arresting the cell cycle from S to G2 phase. In order to assess the mechanisms of HOXA5's effect on cell

cycles, we detected the expression of cyclin A after ectopic expression of HOXA5. The results showed that ectopic expression of HOXA5 significantly reduced the expression of Cyclin A (Figures 3C, 3D). These results suggested that HOXA5 possibly arrested the cell cycle from S to G2 phase through inhibition of the cyclin A expression.

HOXA5 reverses EMT by suppressing the β-catenin/ Snail signaling pathway. The EMT represents a reversible program during which epithelial cells lose their cell identity and acquire a mesenchymal phenotype, and is often associated with the acquisition of cancer migration and invasion [17]. In order to evaluate whether HOXA5 inhibits migration and invasion by reversing EMT, the EMT-related proteins were detected by western blotting. The expression of E-cadherin was increased while the expressions of N-cadherin and Vimentin were decreased when HOXA5 was overexpressed (Figures 4A–4C). These results suggested that HOXA5 may inhibit the migration and invasion of CSCC cells by reversing EMT. The β-catenin/Snail signaling pathway plays an important role in regulating EMT. Overexpression of HOXA5 significantly decreased the expression of β-catenin and Snail by western blotting (Figures 4A–4C). So HOXA5 reversed the EMT process by inhibiting the β-catenin/Snail signaling pathway. The results were also supported by immunohistochemistry assays in human CSCC tissues. Immunohistochemistry results showed that the expression of E-cadherin was mainly localized in the cell membrane and was significantly downregulated in CSCC tissues compared to non-cancerous control tissues ($p<0.05$, Figure 4D). While the expression of N-cadherin, β-catenin, and Snail were upregulated in CSCC tissues. Then we analyzed the relationship between the expression of E-cadherin, N-cadherin, β-catenin, and Snail and HOXA5 in CSCC (Table 2). The expression of HOXA5 was positively correlated with E-cadherin but negatively correlated with N-cadherin. These data suggested that HOXA5 regulated EMT through the β-catenin/Snail signaling pathway.

Overexpression of HOXA5 inhibits the growth of CSCC cells *in vivo*. To investigate the impact of HOXA5 on CSCC *in vivo*, the xenograft tumor model of CSCC cells in nude mice was monitored. SiHa-mCherry-HOXA5 and SiHa-mCherry cells were injected subcutaneously into the nude mice. As shown in Figure 5A–5C, the weight and volume of xenografts tumors derived from SiHa-mCherry-HOXA5 cells were decreased compared to SiHa-mCherry. The expression of EMT-related proteins, β-catenin and Snail, in xenograft tumors was detected by western blotting (Figure 5D). The results showed that the expression of Snail, Vimentin, N-cadherin, and β-catenin were decreased while E-cadherin was increased in SiHa-mCherry-HOXA5 cells derived tumors compared to SiHa-mCherry. Furthermore, the results were also supported by immunohistochemistry (Figure 5E). Ki-67, the cell proliferation marker, was

Table 2. Expression and correlation analysis of HOXA5 with E-cadherin, N-cadherin, β-catenin, and Snail in human CSCC tissue.

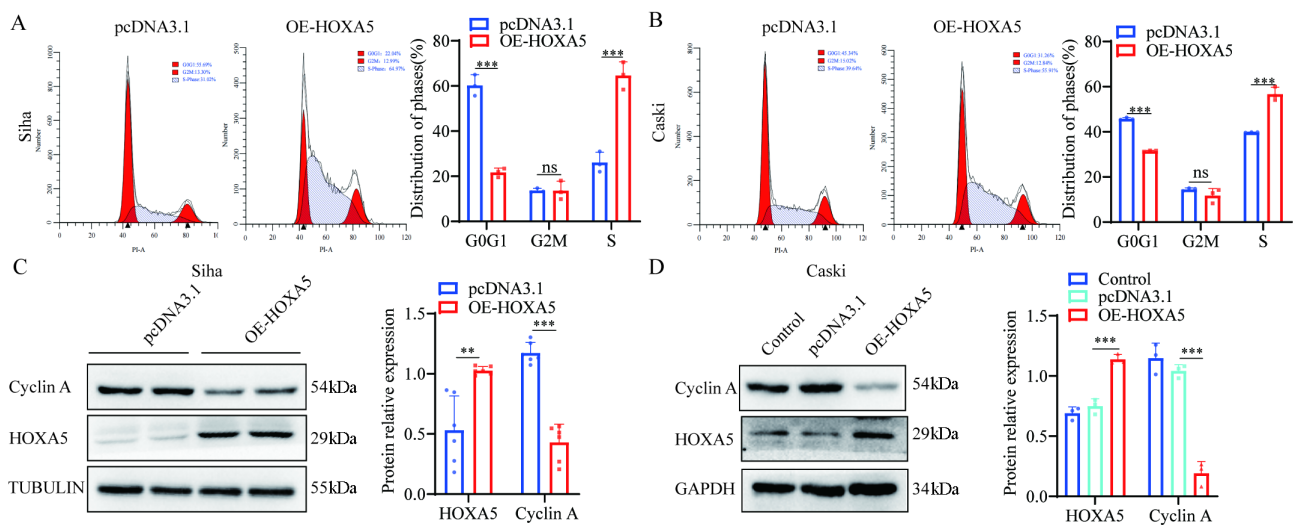| Protein expression in CSCC		HOXA5		p-value	r
		(+) 123	(–) 89		
E-cadherin	(+)	80	46	0.051	0.134
	(–)	43	43		
N- cadherin	(+)	65	32	0.015	0.167
	(–)	58	57		
β-catenin	(+)	89	47	0.003	0.201
	(–)	34	42		
Snail	(+)	89	59	0.345	0.065
	(–)	34	30		

Figure 3. HOXA5 arrests the cell cycle from S to G2 phase. A, B) The cell cycle was tested by flow cytometry after overexpression of HOXA5 in SiHa cells (A) and CaSki cells (B). C, D) The expression of Cyclin A was detected by western blotting in SiHa cells (C) and CaSki cells (D).
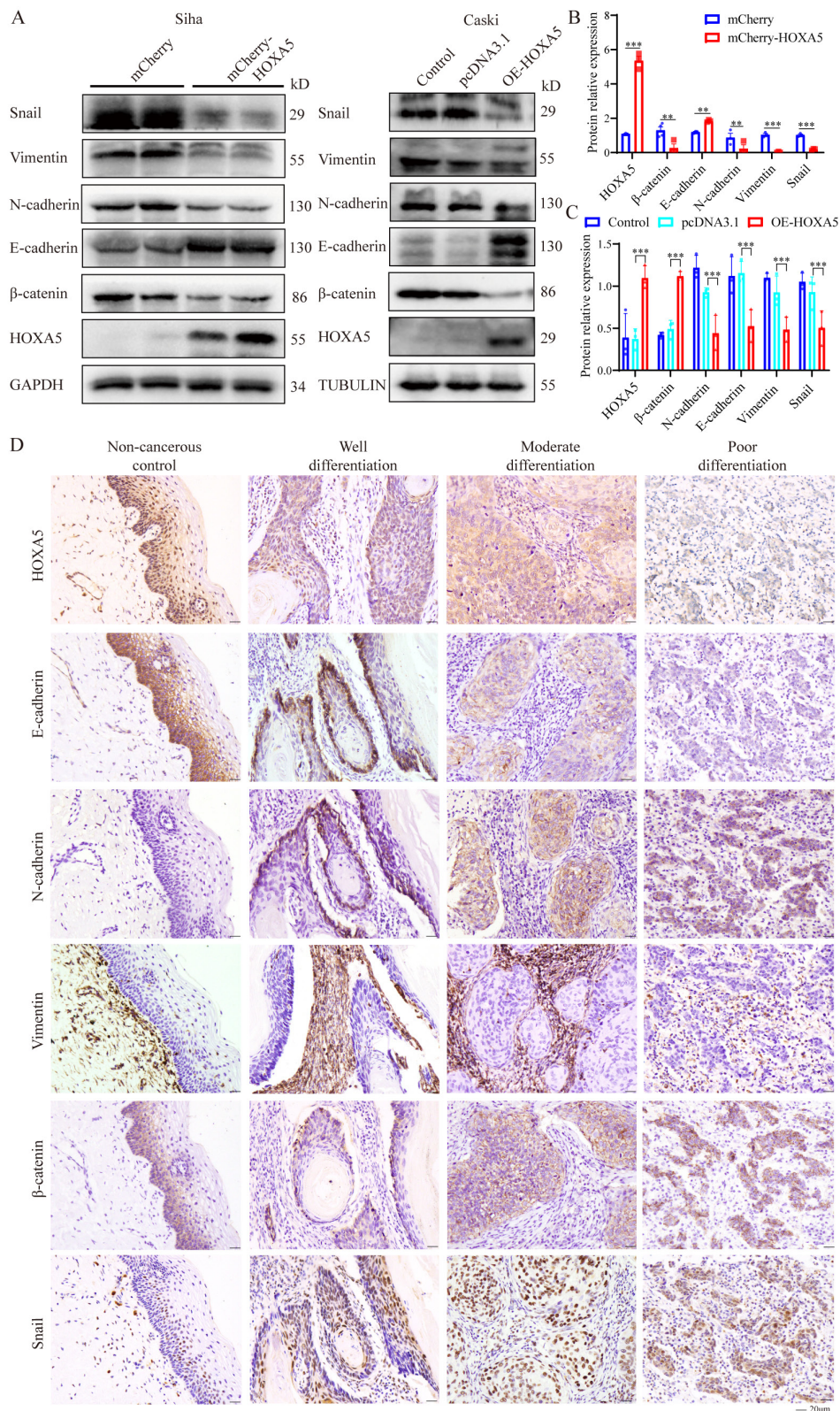
Figure 4. HOXA5 reverses EMT by suppressing the β-catenin/Snail signaling pathway. A) The expression of EMT-associated molecular was detected by western blotting after overexpression of HOXA5 in SiHa and CaSki cells. B, C) Quantitative analysis of protein band gray value was conducted by using Image J software in SiHa (B) and CaSki cells (C). D) The expression of HOXA5, E-cadherin, N-cadherin, Vimentin, β-catenin, and Snail in CSCC and non-cancerous control tissues was tested by immunohistochemistry.
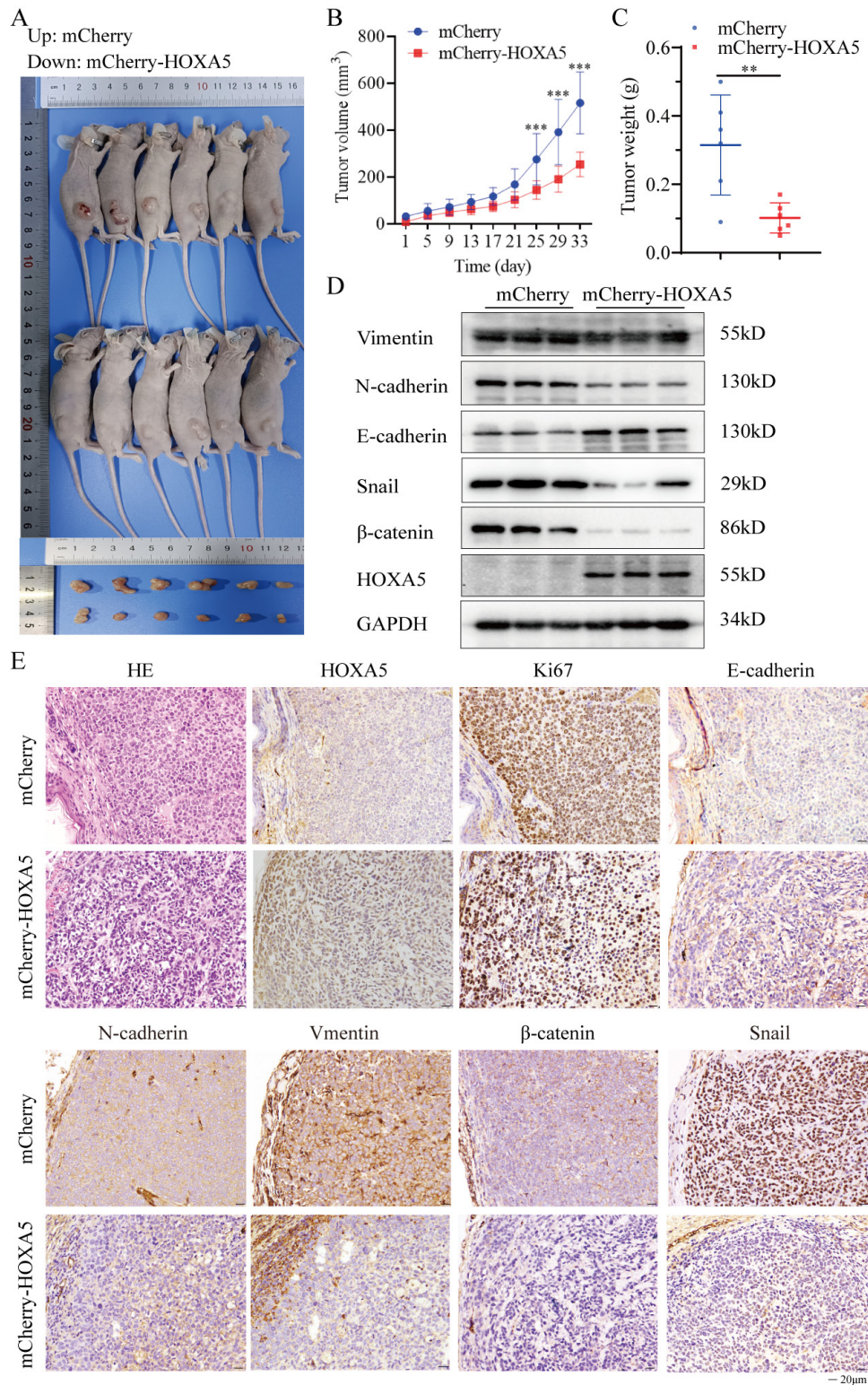
Figure 5. Overexpression of HOXA5 inhibits the growth of CSCC *in vivo*. A) The images of xenograft tumors derived from SiHa-mCherry-HOXA5 cells and SiHa-mCherry cells. **B)** The tumor volumes were recorded every 4 days to evaluate the growth rate of xenograft tumors (n=6). **C)** The weights of xenograft tumors were measured from each group (n=6). **D)** EMT-associated proteins in xenograft tumors derived from SiHa-mCherry cells and SiHa-mCherry-HOXA5 cells were detected by western blotting. **E)** Immunohistochemistry was conducted to evaluate the protein expressions in xenograft tumors.

evaluated by immunohistochemistry assays to evaluate the proliferation ability of SiHa-HOXA5 cells *in vivo*. Tumor tissues from SiHa-mCherry-HOXA5 cells exhibited stronger HOXA5 staining but weaker Ki-67 staining than SiHa-mCherry. These results suggested that HOXA5 inhibited tumor growth *in vivo*.

Overexpression of HOXA5 inhibits the metastasis of CSCC cells *in vivo*. A pulmonary metastasis model was established to test the migration ability of CSCC cells *in vivo*. SiHa-mCherry-HOXA5 and SiHa-mCherry cells were injected in the nude mouse by tail intravenous. The number of pulmonary metastatic nodules derived from SiHa-mCherry-HOXA5 cells was fewer and the sizes of these were smaller than SiHa-mCherry cells (Figures 6A–6C). These results were also confirmed by HE staining (Figure 6B). The expression of E-cadherin was increased while N-cadherin, β-catenin, and Snail were decreased in pulmonary metastatic tumors derived from SiHa-mCherry-HOXA5 cells compared with SiHa-mCherry cells by immunohistochemistry (Figure 6D).

Furthermore, Ki-67 was also decreased in SiHa-mCherry-HOXA5. These results demonstrated that HOXA5 inhibited the metastasis of CSCC cells *in vivo*.

Discussion

Homeobox genes are major transcription factors that regulate tissue and organ development, which have been discovered in Drosophila for the first time [18]. The 39 HOX genes of mammals were respectively assigned to different chromosomes and formed 4 chromosome clusters: HOXA, HOXB, HOXC, and HOXD [19]. The expression of HOXA5 is mainly restricted to the interstitium of the lung, gut, thyroid, breast, and ovary [20]. Several studies have demonstrated that deregulated HOX expression is associated with oncogenesis and HOX expression is closely related to tumor development, invasion, and metastasis [21]. HOXA5 expression was found decreased in many cancers, such as breast cancer, non-small cell lung cancer (NSCLC), colorectal cancer,
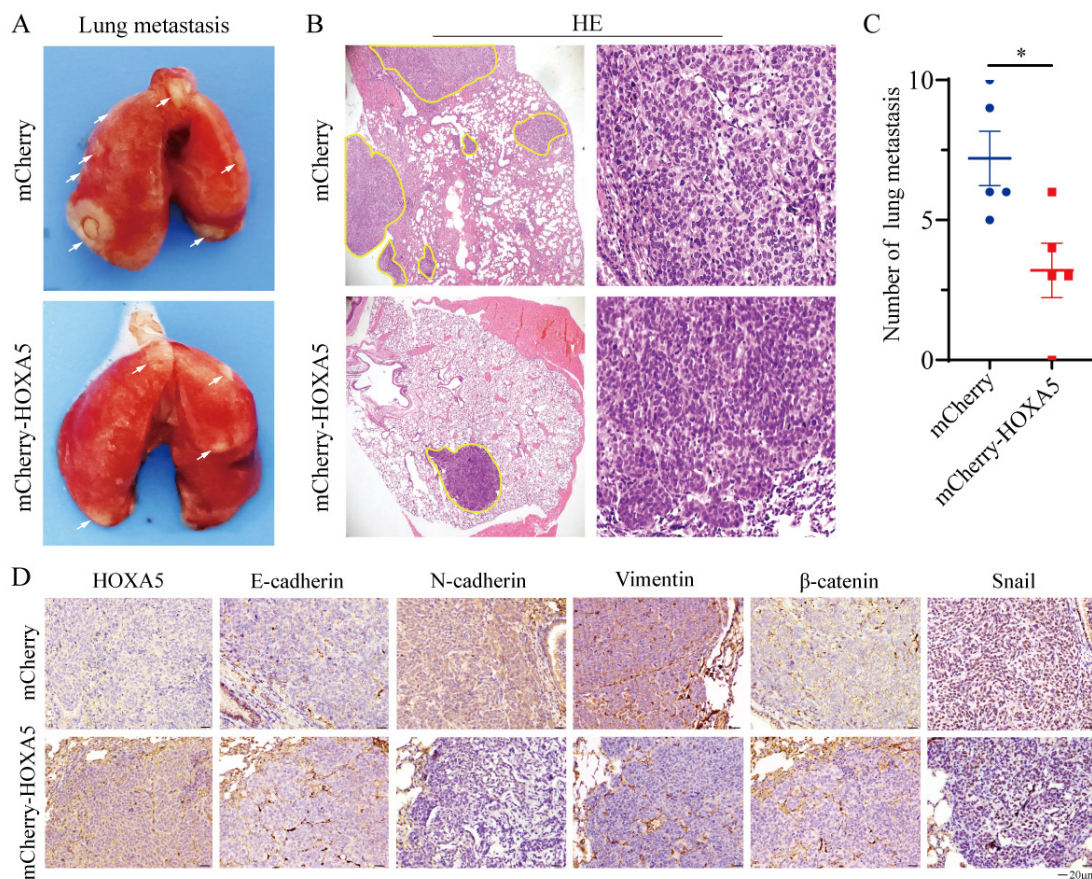

Figure 6. Overexpression of HOXA5 inhibits the metastasis of CSCC cells *in vivo*. A) Typical images of pulmonary metastatic nodules originated from SiHa-mCherry-HOXA5 cells and SiHa-mCherry cells. **B)** HE staining was used to evaluate the number and pathological characteristics of metastatic pulmonary nodules (n=5). **C)** The number of pulmonary metastatic nodules was counted from each group (n=5). **D)** The expression of HOXA5, Ki-67, E-cadherin, N-cadherin, Vimentin, β-catenin, and Snail in metastatic pulmonary nodules originated from SiHa-mCherry-HOXA5 cells and SiHa-mCherry cells was tested by immunohistochemistry.
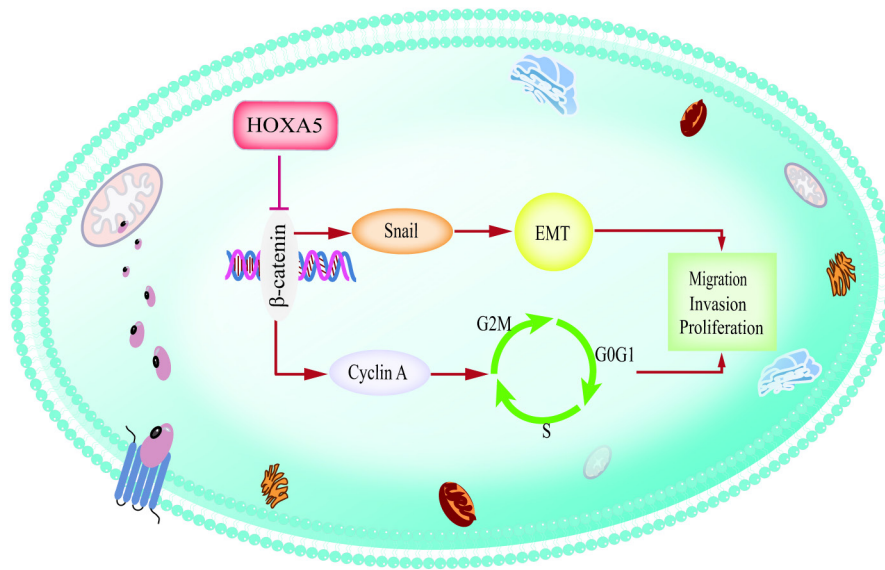
Figure 7. The schematic diagram of HOXA5 inhibiting CSCC progression.

cervical cancer, and gastric cancer [10, 18, 22, 23]. Furthermore, reduced HOXA5 expression correlates with breast cancer progression and is associated with poor prognosis in NSCLC. In our previous study, we found that the expression of HOXA5 was downregulated in CSCC tissues [15]. In this study, we detected the expression of HOXA5 in CSCC and paracancer tissues by immunohistochemistry and western blotting, HOXA5 was highly expressed in paracancer tissues but low or even not expressed in CSCC tissues. These results were consistent with our previous study and suggested that HOXA5 may function as a tumor suppressor.

HOXA5 regulates tumor occurrence and development, mainly by regulation of multiple signaling pathways and transcription factors [21, 24]. In cervical cancer, ectopic expression of HOXA5 arrested the cell cycle from G0/G1 to S phase by inhibiting Cyclin D1 expression and restrained cell proliferation [25]. Overexpression of HOXA5 decelerates the G1-S phase transition and proliferation of gastric cancer cells [26]. In our results, we found that HOXA5 inhibited the proliferation of CSCC cells by arresting the cell cycle process from S to G2/M phase which may relate to Cyclin A. Several studies have shown that HOXA5 regulated the cell cycle dependent on the Wnt/β-catenin pathway. Upregulation of HOXA5 inhibited the progression and metastasis of colorectal cancer by reversing the activation of the Wnt/β-catenin pathway, thereby affecting the changes in intestinal morphology [18]. In cervical cancer, HOXA5 inhibited the activity of the Wnt/β-catenin pathway to repress cell proliferation [25]. Cyclin A is considered to be a downstream factor of the Wnt/β-catenin signaling pathway [27]. In prostate cancer, inhibition of Wnt3/surviving induced cell cycle arrest in the S phase through suppressing Cyclin A3 and Cyclin

B3 [28, 29]. We found that ectopic expression of HOXA5 inhibited the expression of β-catenin and Cyclin A. These results suggested that HOXA5 may inhibit the cell cycle by repressing the β-catenin/Cyclin A signaling pathway.

Complex and variable invasion and metastasis are the main characteristics of malignant tumors [30, 31]. Tumor cells acquire the ability of invasion and metastasis by destroying the adhesion between cells [32]. It is well known that the key step in initiating the cascade of invasion and metastasis is the activation of EMT [33]. When activation of EMT, epithelial cells lose polarity, acquire the properties of mesenchymal cells, and enhance the ability of cell movement, which makes it possible for cancer cells to metastasize [34–36]. The Wnt/β-catenin pathway has been confirmed to play a significant role in the process of EMT [37–39]. Many reports showed that β-catenin is the main regulator of E-cadherin. Moreover, snail plays an important role in tumor metastasis by regulation of EMT [40]. The report showed that β-catenin signaling functions as the snail activator to induce EMT in endometriosis [41]. Wnt/β-catenin/Snail signaling transduction is known to activate the EMT program [42]. In breast cancer, HOXA5 mutation also regulates mammary epithelial cells by reversing EMT [19]. In our study, we found that HOXA5 inhibited the invasion and metastasis of CSCC cells by repressing EMT. Furthermore, HOXA5 repressed the expression of β-catenin and Snail. These results suggested that HOXA5 repressed EMT via the Wnt/β-catenin/Snail signaling pathway in CSCC.

In conclusion, the expression HOXA5 is downregulated in CSCC patients. Overexpression of HOXA5 can inhibit the proliferation, invasion, and metastasis of CSCC cells by repressing the β-catenin/Snail signaling pathway (Figure 7).

Our findings highlight the role and molecular mechanism of HOXA5 in CSCC progression and provide valuable information for clinical practices.

References

[1] ARBYN M, WEIDERPASS E, BRUNI L, DE SANJOSE S, SARAIYA M et al. Estimates of incidence and mortality of cervical cancer in 2018: a worldwide analysis. Lancet Glob Health 2020; 8: e191–e203. https://doi.org/10.1016/S2214-109X(19)30482-6

[2] HASEEB AA, RAHIM AU, IQBAL S, BATOOL H, YOUNAS S et al. The frequency of occult cervical metastasis in oral squamous cell carcinoma patients – A cross sectional study. J Pak Med Assoc 2022; 72: 66–70. https://doi.org/10.47391/JPMA.1512

[3] SIMMS KT, STEINBERG J, CARUANA M, SMITH MA, LEW JB et al. Impact of scaled up human papillomavirus vaccination and cervical screening and the potential for global elimination of cervical cancer in 181 countries, 2020-99: a modelling study. Lancet Oncol 2019; 20: 394–407. https://doi.org/10.1016/S1470-2045(18)30836-2

[4] NAGLE CM, CROSBIE EJ, BRAND A, OBERMAIR A, OEHLER MK et al. The association between diabetes, comorbidities, body mass index and all-cause and cause-specific mortality among women with endometrial cancer. Gynecol Oncol 2018; 150: 99–105. https://doi.org/10.1016/j.ygyno.2018.04.006

[5] DUNN J, SIMMONS R, THABET S, JO H. The role of epigenetics in the endothelial cell shear stress response and atherosclerosis. Int J Biochem Cell Biol 2015; 67: 167–176. https://doi.org/10.1016/j.biocel.2015.05.001

[6] HOBERT O. Homeobox genes and the specification of neuronal identity. Nat Rev Neurosci 2021; 22: 627–636. https://doi.org/10.1038/s41583-021-00497-x

[7] BHATLEKAR S, FIELDS JZ, BOMAN BM. HOX genes and their role in the development of human cancers. J Mol Med (Berl) 2014; 92: 811–823. https://doi.org/10.1007/s00109-014-1181-y

[8] JEANNOTTE L, GOTTI F, LANDRY-TRUCHON K. Hoxa5: A Key Player in Development and Disease. J Dev Biol 2016; 4. https://doi.org/10.3390/jdb4020013

[9] ANBAZHAGAN R, RAMAN V. Homeobox genes: molecular link between congenital anomalies and cancer. Eur J Cancer 1997; 33: 635–637. https://doi.org/10.1016/s0959-8049(97)00010-5

[10] HENDERSON GS, VAN DIEST PJ, BURGER H, RUSSO J, RAMAN V. Expression pattern of a homeotic gene, HOXA5, in normal breast and in breast tumors. Cell Oncol 2006; 28: 305–313. https://doi.org/10.1155/2006/974810

[11] WU Y, ZHOU T, TANG Q, XIAO J. HOXA5 inhibits tumor growth of gastric cancer under the regulation of microRNA-196a. Gene 2019; 681: 62–68. https://doi.org/10.1016/j.gene.2018.09.051

[12] YOO KH, PARK YK, KIM HS, JUNG WW, CHANG SG. Epigenetic inactivation of HOXA5 and MSH2 gene in clear cell renal cell carcinoma. Pathol Int 2010; 60: 661–666. https://doi.org/10.1111/j.1440-1827.2010.02578.x

[13] WANG YF, LIU F, SHERWIN S, FARRELLY M, YAN XG et al. Cooperativity of HOXA5 and STAT3 Is Critical for HDAC8 Inhibition-Mediated Transcriptional Activation of PD-L1 in Human Melanoma Cells. J Invest Dermatol 2018; 138: 922–932. https://doi.org/10.1016/j.jid.2017.11.009

[14] LI D, BAI Y, FENG Z, LI W, YANG C et al. Study of Promoter Methylation Patterns of HOXA2, HOXA5, and HOXA6 and Its Clinicopathological Characteristics in Colorectal Cancer. Front Oncol 2019; 9: 394. https://doi.org/10.3389/fonc.2019.00394

[15] PEI L, WANG ZQ, SHEN J, YANG YZ, TIAN J et al. Expression and clinical significance of HOXA5, E-cadherin, and beta-catenin in cervical squamous cell carcinoma. Int J Clin Exp Pathol 2018; 11: 3091–3096.

[16] ZHANG Y, FENG J, FU H, LIU C, YU Z et al. Coagulation Factor X Regulated by CASC2c Recruited Macrophages and Induced M2 Polarization in Glioblastoma Multiforme. Front Immunol 2018; 9: 1557. https://doi.org/10.3389/fimmu.2018.01557

[17] GEORGAKOPOULOS-SOARES I, CHARTOUMPEKIS DV, KYRIAZOPOULOU V, ZARAVINOS A. EMT Factors and Metabolic Pathways in Cancer. Front Oncol 2020; 10: 499. https://doi.org/10.3389/fonc.2020.00499

[18] ORDONEZ-MORAN P, DAFFLON C, IMAJO M, NISHIDA E, HUELSKEN J. HOXA5 Counteracts Stem Cell Traits by Inhibiting Wnt Signaling in Colorectal Cancer. Cancer Cell 2015; 28: 815–829. https://doi.org/10.1016/j.ccell.2015.11.001

[19] TEO WW, MERINO VF, CHO S, KORANGATH P, LIANG X et al. HOXA5 determines cell fate transition and impedes tumor initiation and progression in breast cancer through regulation of E-cadherin and CD24. Oncogene 2016; 35: 5539–5551. https://doi.org/10.1038/onc.2016.95

[20] HRYCAJ SM, DYE BR, BAKER NC, LARSEN BM, BURKE AC et al. Hox5 Genes Regulate the Wnt2/2b-Bmp4-Signaling Axis during Lung Development. Cell Rep 2015; 12: 903–912. https://doi.org/10.1016/j.celrep.2015.07.020

[21] CARRIO M, ARDERIU G, MYERS C, BOUDREAU NJ. Homeobox D10 induces phenotypic reversion of breast tumor cells in a three-dimensional culture model. Cancer Res 2005; 65: 7177–7185. https://doi.org/10.1158/0008-5472.CAN-04-1717

[22] ZHANG ML, NIE FQ, SUN M, XIA R, XIE M et al. HOXA5 indicates poor prognosis and suppresses cell proliferation by regulating p21 expression in non small cell lung cancer. Tumour Biol 2015; 36: 3521–3531. https://doi.org/10.1007/s13277-014-2988-4

[23] YAICHE H, TOUNSI-KETTITI H, BEN JEMII N, JABALLAH GABTENI A, MEZGHANNI N et al. New insights in the clinical implication of HOXA5 as prognostic biomarker in patients with colorectal cancer. Cancer Biomark 2021; 30: 213–221. https://doi.org/10.3233/CBM-201758

[24] KACHGAL S, MACE KA, BOUDREAU NJ. The dual roles of homeobox genes in vascularization and wound healing. Cell Adh Migr 2012; 6: 457–470. https://doi.org/10.4161/cam.22164

[25] MA HM, CUI N, ZHENG PS. HOXA5 inhibits the proliferation and neoplasia of cervical cancer cells via downregulating the activity of the Wnt/beta-catenin pathway and transactivating TP53. Cell Death Dis 2020; 11: 420. https://doi.org/10.1038/s41419-020-2629-3

[26] PENG X, ZHA L, CHEN A, WANG Z. HOXA5 is a tumor suppressor gene that is decreased in gastric cancer. Oncol Rep 2018; 40: 1317–1329. https://doi.org/10.3892/or.2018.6537

[27] SHI Y, GE C, FANG D, WEI W, LI L et al. NCAPG facilitates colorectal cancer cell proliferation, migration, invasion and epithelial-mesenchymal transition by activating the Wnt/beta-catenin signaling pathway. Cancer Cell Int 2022; 22: 119. https://doi.org/10.1186/s12935-022-02538-6

[28] ZHAO ZQ, WU XJ, CHENG YH, ZHOU YF, MA XM et al. TROAP regulates cell cycle and promotes tumor progression through Wnt/beta-Catenin signaling pathway in glioma cells. CNS Neurosci Ther 2021; 27: 1064–1076. https://doi.org/10.1111/cns.13688

[29] YE J, CHU C, CHEN M, SHI Z, GAN S et al. TROAP regulates prostate cancer progression via the WNT3/survivin signalling pathways. Oncol Rep 2019; 41: 1169–1179. https://doi.org/10.3892/or.2018.6854

[30] YU H, YE W, WU J, MENG X, LIU RY et al. Overexpression of sirt7 exhibits oncogenic property and serves as a prognostic factor in colorectal cancer. Clin Cancer Res 2014; 20: 3434–3445. https://doi.org/10.1158/1078-0432.CCR-13-2952

[31] GUPTA GP, MASSAGUE J. Cancer metastasis: building a framework. Cell 2006; 127: 679–695. https://doi.org/10.1016/j.cell.2006.11.001

[32] CHAFFER CL, WEINBERG RA. A perspective on cancer cell metastasis. Science 2011; 331: 1559–1564. https://doi.org/10.1126/science.1203543

[33] PUISIEUX A, BRABLETZ T, CARAMEL J. Oncogenic roles of EMT-inducing transcription factors. Nat Cell Biol 2014; 16: 488–494. https://doi.org/10.1038/ncb2976

[34] THIERY JP, ACLOQUE H, HUANG RY, NIETO MA. Epithelial-mesenchymal transitions in development and disease. Cell 2009; 139: 871–890. https://doi.org/10.1016/j.cell.2009.11.007

[35] THIERY JP, SLEEMAN JP. Complex networks orchestrate epithelial-mesenchymal transitions. Nat Rev Mol Cell Biol 2006; 7: 131–142. https://doi.org/10.1038/nrm1835

[36] NAWSHAD A, LAGAMBA D, POLAD A, HAY ED. Transforming growth factor-beta signaling during epithelial-mesenchymal transformation: implications for embryogenesis and tumor metastasis. Cells Tissues Organs 2005; 179: 11–23. https://doi.org/10.1159/000084505

[37] WHITE BD, CHIEN AJ, DAWSON DW. Dysregulation of Wnt/beta-catenin signaling in gastrointestinal cancers. Gastroenterology 2012; 142: 219–232. https://doi.org/10.1053/j.gastro.2011.12.001

[38] VALENTA T, HAUSMANN G, BASLER K. The many faces and functions of beta-catenin. EMBO J 2012; 31: 2714–2736. https://doi.org/10.1038/emboj.2012.150

[39] GONZALEZ DM, MEDICI D. Signaling mechanisms of the epithelial-mesenchymal transition. Sci Signal 2014; 7: re8. https://doi.org/10.1126/scisignal.2005189

[40] WANG Y, SHI J, CHAI K, YING X, ZHOU BP. The Role of Snail in EMT and Tumorigenesis. Curr Cancer Drug Targets 2013; 13: 963–972. https://doi.org/10.2174/15680096113136660102

[41] XIONG W, ZHANG L, LIU H, LI N, DU Y et al. E2-mediated EMT by activation of beta-catenin/Snail signalling during the development of ovarian endometriosis. J Cell Mol Med 2019; 23: 8035–8045. https://doi.org/10.1111/jcmm.14668

[42] LIANG G, FANG X, YANG Y, SONG Y. Silencing of CEMIP suppresses Wnt/beta-catenin/Snail signaling transduction and inhibits EMT program of colorectal cancer cells. Acta Histochem 2018; 120: 56–63. https://doi.org/10.1016/j.acthis.2017.11.002